

9th International Conference on Materials Structure and Micromechanics of Fracture

# On the link between as-built surface quality and fatigue behavior of additively manufactured Inconel 718

Radomila Konečná<sup>a\*</sup>, Gianni Nicoletto<sup>b</sup>

<sup>a</sup>University of Žilina, Faculty of Mechanical Engineering, Department of Materials Engineering, Univerzitná 8215/1, 010 26 Žilina, Slovakia

<sup>b</sup>University of Parma, department of Engineering and Architecture, Parco Area della Scienze 181/A, 43124 Parma, Italy

---

## Abstract

Inconel 718 is widely used in challenging structural applications because of its excellent high temperature mechanical properties. Selective Laser Melting (SLM) of Inconel 718 powder is increasingly used to fabricate customized parts for jet engines. The surface quality of SLM parts is influenced by powder characteristics, process parameters and the layer-wise fabrication. The as-built fatigue behavior is negatively affected by the inferior surface quality of SLM parts compared to machined version. Here the fatigue behavior of SLM Inconel 718 is investigated using specimens fabricated with two different SLM systems and different directions of applied stress with respect to build direction. Fatigue test results are interpreted in the light of metallographic and fractographic investigations.

© 2019 The Authors. Published by Elsevier B.V.

This is an open access article under the CC BY-NC-ND license (<http://creativecommons.org/licenses/by-nc-nd/4.0/>)

Peer-review under responsibility of the scientific committee of the ICMSMF organizers

*Keywords:* Type your keywords here, separated by semicolons ;

---

## 1. Introduction

Inconel 718 is a Ni-based superalloy widely used in hot structures of jet engines, because of its excellent mechanical properties at high temperatures and its good weldability. This material has been extensively studied in cast and wrought forms during the past decades. Recently, customized parts of complex geometry are increasingly fabricated by Selective Laser Melting (SLM) of Inconel 718 powder, Clark et al. (2008). The SLM process, one of the most widely

---

\* Corresponding author. Tel.: +0-421-513-2604; fax: +0-000-000-0000 .

E-mail address: [radomila.konecna@fstroj.uniza.sk](mailto:radomila.konecna@fstroj.uniza.sk)

used metal additive manufacturing technologies, enables the production of metallic components directly from a computer-aided design (CAD) file of unlimited complexity by localized powder melting layer after layer by a concentrated laser beam.

The microstructure of SLM Inconel 718 is substantially different from that of conventionally manufactured materials because of the typical rapid solidification. The layer-by-layer process typically adopts a contour and hatch strategy of the laser motion that generates a columnar microstructure. Nonetheless, the static mechanical properties are found to be comparable in terms of the ultimate strength, yield strength and elongation to conventional processed materials, Wells (2016).

In general, the fatigue properties of SLM metals vary considerably according to the processing parameters because they affect the microstructure, porosity content, residual stresses and relatively rough part surfaces. Part performance in fatigue is therefore significantly lower compared to machined counterparts. Quantification and understanding of this fatigue gap is a fundamental step in SLM process qualification, Yadollahi and Shamsaei (2017).

The aim of this contribution is establishing a link between SLM fabrication and fatigue performance of as-built Inconel 718. Since SLM process parameters, such as layer thickness and laser power, and printing strategy influence the as-built surface quality, surface and subsurface features plays a fundamental role on the fatigue behavior in terms of damage localization and initiation mechanisms. Therefore, here specimens with as-built surfaces produced with two different SLM systems and oriented in two different directions with respect to build direction are tested in fatigue. Then surface roughness and near surface microstructure of the directional fatigue specimens are investigated on etched metallographic sections. Finally, a fractographic investigation is performed to link specimen orientations and production systems to fatigue crack initiation localization and mechanisms.

## 2. Experimental details

**SLM processing of Ni-based alloy.** The material of this study is gas atomized Inconel 718 alloy powder of controlled granulometry. The chemical composition was determined by spectrometry and was the following:

Table 1. Chemical composition of IN 718 powder.

Element	Ni	Cr	Fe	Nb	Mo	Co	Ti	Al	Cu
Wt. %	51.56	17.9	18.2	5.23	3.21	0.15	1.14	2.19	0.05

Two different SLM systems operated by service provider BEAM-IT (Fornovo Taro, Italy) were used to manufacture different sets of fatigue specimens: an older Renishaw AM 250 system (Renishaw, UK) operated to layer thickness of 30  $\mu\text{m}$  and a more recent SLM Solution M280QL system (SLM Solutions, Germany) operated to layer thickness of 50  $\mu\text{m}$ . The process parameters of the two systems were defined after optimization and qualification phases managed by BEAM-IT. The layer-wise powder transformation by selective laser melting was carried out in an Argon atmosphere with built plate temperature maintained at 200  $^{\circ}\text{C}$ .

The SLM fabrication with the two systems occurred at different times but the post-processing steps were the same: that is heat treatment before specimen removal from the base plate and a two-step heat treatment after removal given by: i) stress relief (solution with heating to 970  $^{\circ}\text{C}$  for 1 hour followed by cooling in Argon atmosphere) ii) age hardening by double aging (heating to 710  $^{\circ}\text{C}$  and holding for 8 hours, further aged at 610  $^{\circ}\text{C}$  for 8 hours and final cooling to room temperature in Argon).

Structural and failure characterization. Metallographic specimens were prepared according to standard techniques and then observed using the Neophot 32 light microscope and Tescan LYRA 3 XMU FEG/SEM with EDX analysis system. Microstructure was analyzed after etching with Kalling's reagent (2 g of  $\text{CuCl}_2$ , 40 ml of  $\text{HCl}$ , 80 ml of methanol).

The Vickers hardness measurement after aging was performed using the 250 HPO/AQ apparatus. The load of 98.1 N was applied for 10 s. The average hardness value of 483 HV10 was determined for Renishaw and 489 HV10 was determined for SLM 280HL system. The hardness did not show dependence on specimen orientation and did not show differences depending of used AM system.

After the fatigue tests, broken specimens were investigated in the SEM with the aim of determining location and number of initiation places and investigating the micromechanism of fatigue crack initiation and evolution.

**Fatigue testing.** The role of the as-built surface quality on the fatigue strength was the aim of a test campaign. Specifically, two stress directions, perpendicular and parallel to the layers, were investigated. A special miniature prismatic specimen geometry introduced in Nicoletto (2017) was adopted to investigate the directional effect on fatigue. Fig. 1 shows the different specimen directions with respect to build direction and their denomination. The size of the nominal section is  $5 \times 5 \text{ mm}^2$  and the specimen length is 22 mm. The arrows on the flat surfaces show the direction of the applied cyclic stress. The present test methodology has been already extensively used, Nicoletto (2018). The specimen loading is cyclic bending with a stress ratio  $R = 0$  and a frequency of 20 Hz. Test run-out was fixed at  $2 \times 10^6$  cycles.

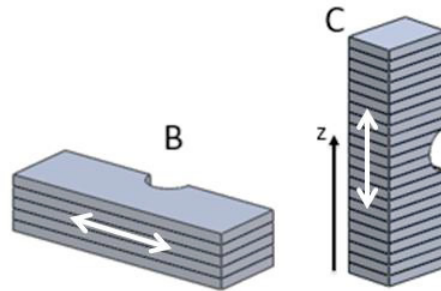


Fig. 1. Mini specimen orientations with respect to build direction. White arrow defines the applied stress direction.

To account for the nonstandard specimen geometry, the following factor  $C_{mg} = \sigma_{eff} / \sigma_{nom} = 0.91$ , determined by elastic finite element analysis, Nicoletto (2017), is used to convert the nominal maximum bending stress into the effective maximum stress. The effective stress is used to compare miniature specimen fatigue data to standard smooth specimen fatigue data.

### 3. Results and discussion

This section presents initially the results of the fatigue characterization of as-built Inconel 718 produced by the two SLM systems. Then an explanation of the observed fatigue behavior is sought using a characterization of the as-built surface quality of the different specimens.

**Fatigue behavior.** The high cycle fatigue data (maximum effective cyclic stress vs. number of cycles) of the two orientations of miniature specimens produced by the two SLM systems are plotted together in Fig. 2.

The scatter of the individual four data sets is rather low suggesting that the as-built surface quality has a stable effect. The trends in a linear-log plot are well behaved and similar although shifted one with respect to the others.

The influence of SLM system and layer thickness is well defined: the SLM 280HL at  $50 \mu\text{m}$  layer thickness gives a better fatigue behavior than the Renishaw AM250 at  $30 \mu\text{m}$  layer thickness. Since the specimen surfaces were flat the layer thickness affected only the fabrication rate. In the case of curved surfaces, the thinner layer may obtain a better resolution of the desired geometry.

Independently of the AM system, the fatigue behavior of as-built Inconel 718 is significantly directional. However, the two AM systems result in two different directional responses in fatigue. Namely, for Renishaw AM 250 the perpendicular direction to layers is weaker compare to the parallel direction while the opposite holds for SLM 280HL, where the fatigue strength in the direction perpendicular to layers is higher than the parallel direction. Interestingly, the ranking obtained in a previous study of DMLS Ti6Al4V was different with Type C direction having the worst fatigue performance, Nicoletto (2018). The effective strengths at  $2 \times 10^6$  cycles can be estimated:  $\sigma_{max, 2 \times 10^6} = 455 \text{ MPa}$  for Type C;  $\sigma_{max, 2 \times 10^6} = 365 \text{ MPa}$  for Type B for the SLM 280HL and  $\sigma_{max, 2 \times 10^6} = 340 \text{ MPa}$  for Type B;  $\sigma_{max, 2 \times 10^6} = 260 \text{ MPa}$  for Type C for Renishaw AM250.

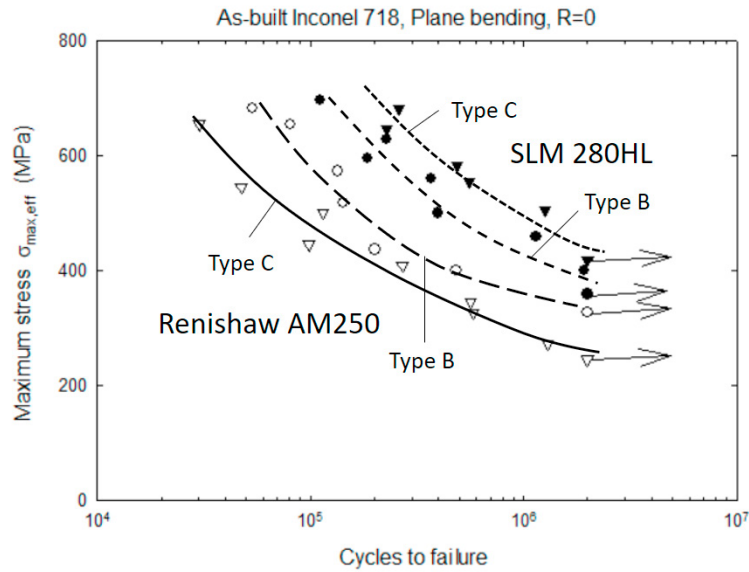


Fig. 2. Directional fatigue behavior of as-built and heat treated SLM Inconel 718 produced with the two SLM systems.

These data can be compared to a thorough study of as-built SLM Inconel 718 fabricated with a Concept Laser system, Wells (2016). Fatigue testing of two axial specimen directions (i.e. parallel to build and at  $45^\circ$  to build) determined fatigue strengths at  $2 \times 10^6$  cycles ranging from 300 MPa to 400 MPa. The agreement of the two independent test programs is therefore quite good.

**As-built surface characterization.** Longitudinal cross-sectional views of the as-built fatigue specimen surfaces produced by the two SLM systems are shown in Fig. 3. The quality of the near-surface material depends on the operating parameters of the two SLM systems. On the other hand, the fatigue performance is the result of the interaction of such near surface material features and the applied cyclic stress for the different specimen orientations defined in Fig. 1.

Table 2. Roughness vs fatigue specimen type and SLM system.

	Renishaw AM250		SLM 280HL	
	Type B	Type C	Type B	Type C
$R_a$ [ $\mu\text{m}$ ]	10.67	15.56	4.41	4.10
$R_z$ [ $\mu\text{m}$ ]	56.96	84.43	36.40	32.97

Inspection of Fig. 3 shows qualitatively that the surface roughness obtained with the Renishaw AM 250 system is greater than in the case of the SLM 280HL system for both types of specimens. To quantify these differences, roughness measurements of parameters  $R_a$  and  $R_z$  were performed for the different specimens prepared with the two SLM systems and are presented in Table 2. The roughness of the Renishaw system is considerably larger than that of SLM 280HL system. The difference depends on the roughness parameter i.e. approx. three times in terms of  $R_a$  and about twice in terms of  $R_z$ .

The average roughness measures  $R_a$  and  $R_z$  of Renishaw specimens are different for the different orientations, namely Type C roughness is greater (i.e. about 50 %) than Type B roughness. On the other hand, the roughness measures  $R_a$  and  $R_z$  of SLM 280HL specimens are quite similar for the two orientations. Interestingly in this case, Type B roughness is only slightly greater (i.e. about 10 %) than Type C roughness. The surface roughness measurements of Table 2 inversely correlate with the experimental fatigue ranking of Fig. 2. That is the fatigue strength of Type C SLM 280 HL is the highest and the Type C Renishaw AM250 is the lowest. However, surface roughness may not be the unique feature responsible of the directional fatigue behavior determined in Fig. 2.

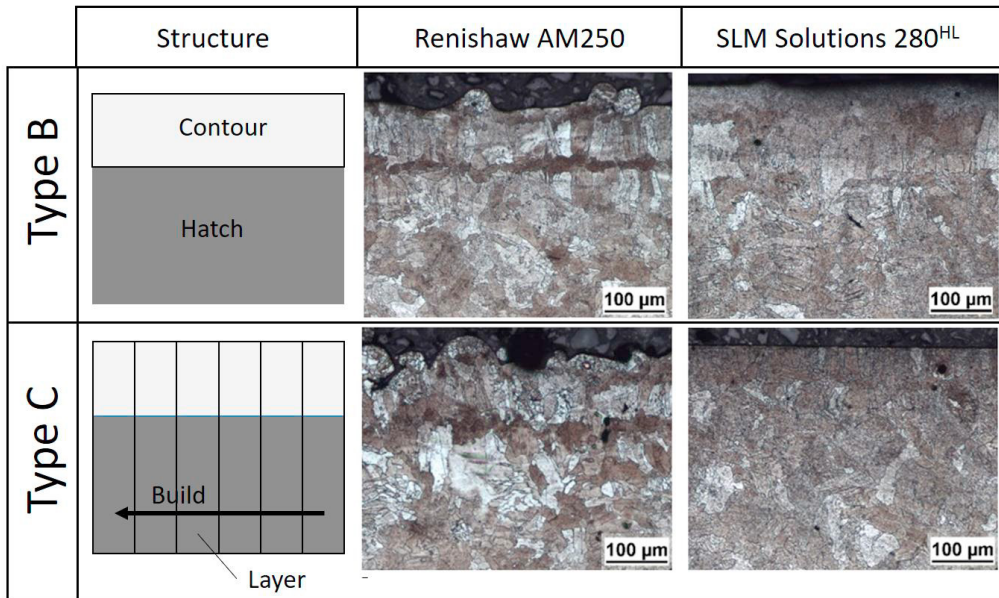


Fig. 3. Cross sections of as-built surfaces for the different specimens and the two AM systems and associated structure.

Well known is the role of sub surface defects on early fatigue crack initiation, Deng et al. (2018) SLM fabrication typically adopts a layer-wise strategy involving a raster laser motion and melting of the inner areas (i.e. hatching) and the layer contouring. Process parameters (i.e. energy, speed etc.) are typically different because of the different requirements of high productivity for the internal volume and accuracy and smoothness of the part surface. When producing directional fatigue specimens such as those of Fig. 1, the near surface layers subjected to cyclic stress are affected in a different way by the printing strategy. Fig. 3 schematically shows contour and hatching in the different specimen types along the etched cross-sections. The near-surface microstructures clearly show heterogeneity and directionality. Further, the surface roughness of Type B specimens is mainly affected by the contour parameters while the roughness of Type C specimens has a contribution from the sequence of contour cross-sections.

**Fatigue crack initiation.** Fatigue cracks initiate at or near that rough flat surface of the directional bending specimens of Fig. 1 subjected to a pulsating tensile stress (i.e.  $R = 0$ ). Surface roughness values are given in Tab. 2. The key factors for the initiation of fatigue cracks is the stress level and its interaction with local surface defects. Multiple fatigue crack initiation was identified in specimens produced with both AM systems.

Examination of fatigue fracture surfaces with the SEM revealed typical fatigue initiation sites shown in Fig. 4. Type B specimens are stressed in the direction parallel to the layer. Fig. 4a (Renishaw) and Fig. 4c (SLM Solutions) show incomplete inter-layer melting where crack initiation occurred. On the other hand, Type C specimens are stressed in the direction perpendicular to the layers. Therefore, Fig. 4b (Renishaw) and Fig. 4d (SLM Solutions) show localized crack initiation at stress concentrations due to non-melted powder particles and a local structural defects. The smoother surface and small defects of Fig. 4d correlate with a better fatigue performance when compared to the rougher surface of Fig. 4b.

#### 4. Conclusions

- Fabrication parameters and print strategy of an SLM system significantly influence the fatigue response of as-built Inconel 718.
- As-built fatigue behavior of SLM Inconel 718 is influenced by the direction of the applied stress with respect to build direction (i.e. anisotropic).
- The effective fatigue strength ( $\sigma_{\max}$  at  $2 \times 10^6$  cycles at  $R = 0$ ) of as-built SLM Inconel 718 ranges from 260 MPa to 455 MPa depending on SLM system and stress orientation.
- The fatigue crack initiation depends on the interaction of the stress and the surface roughness and near surface microstructure.

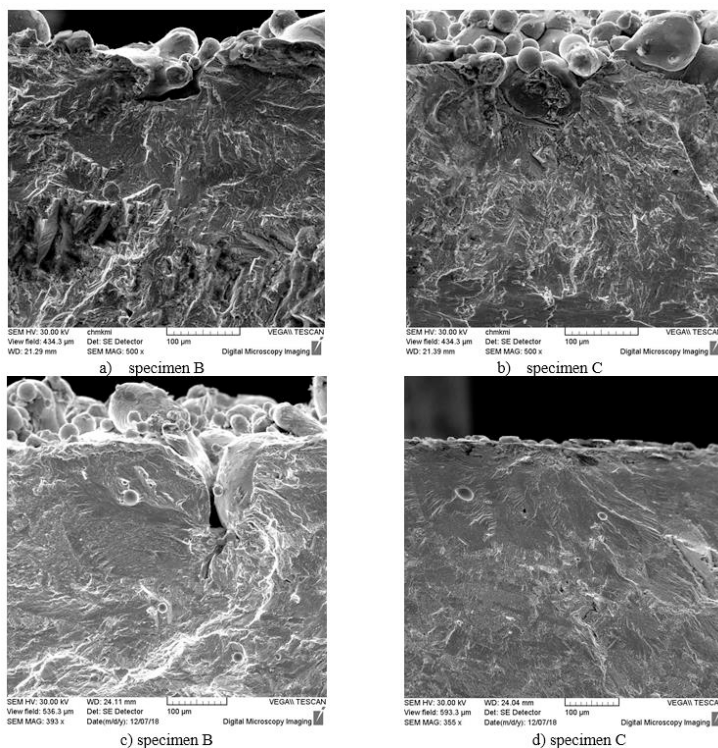


Fig. 4. Places of crack initiation a), b) Renishaw AM250 and c), d) SLM 280 HL production.

## Acknowledgements

The authors acknowledge the company BEAM-IT srl, Fornovo Taro, Italy for providing the specimens and the VEGA grant agency for the support by the grant No. 1/0463/19.

## References

- Clark, D., Bache, M.R., Whittaker, M.T., 2008. Shaped metal deposition of a nickel alloy for aero engine applications. *Journal of Materials Processing Technology* 203,39–448.
- Deng, D., Peng, R.L., Brodin, H., Moverare, J., 2018. Microstructure and mechanical properties of Inconel 718 produced by selective laser melting: Sample orientation dependence and effect of post heat treatments. *Materials Science & Engineering A* 713, 294–306.
- Nicoletto, G., 2017. Anisotropic high cycle fatigue behavior of Ti-6Al-4V obtained by powder bed laser fusion. *International Journal of Fatigue*, vol. 94, pp. 255-262.
- Nicoletto, G., Directional and notch effects on the fatigue behavior of as-built DMLS Ti6Al4V, *International Journal of Fatigue*, 106 (2018) pp. 124-131.
- Wells, D., 2016. Overview of fatigue and damage tolerance performance of powder bed fusion alloy N07718. *ASTM/NIST Workshop on Mechanical Behavior of Additive Manufactured Components*, San Antonio, Texas, NASA Report No. 20160007069.
- Yadollahi, A., Shamsaei, N., 2017. Additive manufacturing of fatigue resistant materials: Challenges and opportunities, *International Journal of Fatigue*, 9814–31.